J Intell Robot Syst (2008) 51:421–438
DOI 10.1007/s10846-007-9195-0

Adjustment of Home Posture of Biped Humanoid Robot Using Sensory Feedback Control

Jung-Hoon Kim · Jung-Yup Kim · Jun-Ho Oh

Received: 31 July 2007 / Accepted: 13 November 2007 /
Published online: 21 February 2008

Abstract Humanoid robot dynamic walking is seriously affected by the initial home posture (walking ready posture). If the initial home posture is not accurate, the robot may fall down during walking despite using robust walking control algorithm. Moreover, the initial home posture of a real physical robot is slightly different at every setting because the zero position of the joint is not exactly the same. Therefore, an accurate and consistent initial home posture is essential when we compare and analyze walking control algorithms. In order to find a zero position, an incremental encoder with a limit switch or an absolute encoder such as a potentiometer can generally be used. However, the initial calibration of this method for a multi-axis humanoid robot that enables the desired initial sensor signal is difficult and time-consuming. Furthermore, it has the disadvantage that additional limit switches or absolute encoders can interfere with the design objective of compactness. Therefore, this paper describes a novel adjustment method of the home posture for a biped humanoid robot utilizing incremental encoders, an inertial sensor and force torque sensors. Four kinds of controllers are proposed for the adjustment of the home posture and adjusted offsets are measured when the outputs of the controllers have converged. Experimental results from KHR-2 show the effectiveness of the proposed adjustment algorithm.

J.-H. Kim (✉)
Intelligent Robot Laboratory, Department of Mechanical Engineering, Myongji University,
San 38-2 Namdong, Cheoin-Gu, Yongin, Gyeonggi-Do 449-728, South Korea
e-mail: maysmile@gmail.com

J.-Y. Kim · J.-H. Oh
HUBO Laboratory, Humanoid Robot Research Center, Department of Mechanical Engineering,
Korea Advanced Institute of Science and Technology, 373-1 Guseong-dong Yuseong-gu,
Daejeon 305-701, South Korea

J.-Y. Kim
e-mail: jungyupkim@kaist.ac.kr

J.-H. Oh
e-mail: jhoh@kaist.ac.kr

Keywords Home posture · Biped walking robot · Practical adjustment · Inertial sensor · Force torque sensor

1 Introduction

Research on humanoid robots has been increasing since the successful debut of the Honda humanoid robot [1]. Humanoid robotics research can be classified into mobility, manipulation, navigation, intelligence, and interaction. Among these, dynamic biped walking control is related to mobility, and it is fundamental research for realizing a humanoid robot that can move in a human environment.

The Humanoid Research Center in KAIST has developed humanoid robots since 2001 [2–7]. KHR-1(KAIST Humanoid Robot Platform-1) was the first platform for testing biped walking capability [2–4]. After achieving successful dynamic walking, we designed the second platform KHR-2, which has an enhanced control architecture based on a distributed control system using a CAN (Controller Area Network) [5]. It can walk, climb stairs, and perform visual tracking using a single CCD camera. HUBO is our third platform. It has a beautiful appearance and a strong mechanical structure. It can change step length and walking frequency while walking and can perform upper body motions based on Fast Fourier Transform and human motion capture [6].

As essential sensors for walking, many humanoid robots are equipped with an inertial sensor on the torso and force torque sensors at the bottom of each feet. In order to measure the joint angle, an incremental encoder, absolute encoder or potentiometer can be used. For an incremental encoder, a limit switch or index pulse is necessary to set a zero position of the joint. An absolute encoder, it does not need a limit switch, but generally its resolution is lower than that of an incremental encoder. A potentiometer signal can drift according to the temperature. Ideally, if the robot is moved into the home posture under position control after setting the zero position of each joint, the upper body angle from an inertial sensor should be zero and the weight on the each foot should be same. However, in reality, it is hard for a multi-axis robot to achieve an ideal home posture and foot force condition because of the accumulated errors of all joints. These accumulated errors are composed of two things. One is an error due to an inaccurate zero position of the joint. The other is a position control error of the joint. In this paper, the authors only address an error from an inaccurate zero position of the joint because it cannot be eliminated by using excellent joint position controller. In order to adjust the home posture, we can modify the initial angles of all joints to realize zero upper body angle and the same weight on the each foot through a trial and error method, but this is not only hard but also time-consuming since there are so many axes on a humanoid robot. In addition, a compact design of a humanoid robot cannot be achieved by attaching limit switches on all robot joints.

If the initial ZMP(Zero Moment Point) [7] is not located at the ideal point due to incorrect zero positions, the actual robot's pose does not perfectly correspond with the desired pose derived by the inverse kinematics solution. Under this condition, the robot becomes unstable when it walks or will have limited walking performance. Improving the accuracy and repeatability of the home posture is very important not only for walking performance but also for developing the walking control algorithm since constant experimental conditions help consistent experimental results.

In robot manipulation, several kinds of kinematic calibration methods have been developed to improve position accuracy. Some researchers constructed an external system that measures the absolute position of the end-point of a manipulator and modified the parameters that define the kinematic model [8–9]. Without measuring the end-point position externally, the calibration method using a triaxial accelerometer fixed to the robot end-point was also proposed [10]. In the field of legged robots, kinematic calibration of a four-legged robot which has a 2-DOF leg was proposed to reduce the foot and body positioning error [11]. However, it is an offline computing method using an iterative optimization algorithm. They could not develop online methods because of hardware limitations. In the field of biped humanoid robots, the effective calibration method has not been made public until now in spite of its importance for walking stability. Therefore, this paper proposes an important adjustment method of home posture for humanoid robots using an inertial sensor and force torque sensors. We introduce four kinds of controllers to find offsets and adjust the initial home posture. They are the ZMP Regulation Controller (ZRC), Orientation Correction Controller (OCC), Compliance Controller (CC), and Ankle Torque Difference Controller (ATDC). ZMP regulation controller (ZRC) is for adjusting ZMP offsets in the transverse plane. It regulates the measured ZMP at the ideal ZMP by changing the pelvis offset position in the Cartesian space. Orientation correction controller (OCC) is introduced to correct the pitch and roll angle of the torso in both sagittal and coronal planes. Using an inertial sensor to measure the direction of gravity, it corrects the roll and pitch pose by changing pitch angles of the ankle and the relative leg length of the left and right legs. If we control the position of a biped robot with the inaccurate initial offsets, feet of the robot do not fully contact the ground during double support due to the offsets and it affects on the overall convergence of the adjustment algorithms. In this situation, backdrivability on the ankle joint is helpful. So, compliance control (CC) is adopted to increase the back-drivability on the roll ankle joint. For the full contact of the feet along the pitch axis, the ankle torque difference controller (ATDC) is proposed and it makes the two torque values on the pitch ankles equal. As a result, the proposed adjustment method enables consistent walking without additional limit switches or absolute encoders.

This paper is organized as follows: In Section 2, we briefly introduce the robot platform of KHR-2. Section 3 describes an adjustment algorithm. Section 4 presents the experimental results of the adjustment algorithm. Finally, in Section 5, we conclude the paper with discussion and future work.

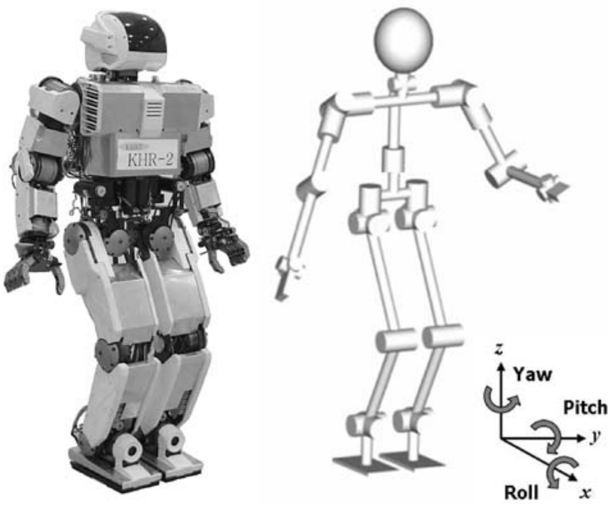

Fig. 1 Photograph of the biped humanoid robot KHR-2 and its joint structure

2 Platform Description

2.1 Mechanical Hardware

In 2003, the authors developed KHR-2, the second version of our biped humanoid robot (Fig. 1). For a human-friendly intelligent robot, we designed it to be the size of a child and gave it sufficient joints to imitate human motions. The weight, height and D.O.F (degrees of freedom) of KHR-2 are 56 kg, 120 cm and 41 (six for each leg, four for each arm, seven for each hand, one for the torso and six for the head) respectively [5]. All joint actuators are brushed DC motors with harmonic reduction gears or planetary gears. We achieved a self-contained system by putting all mechanical and electronic parts into the robot body. Hence, KHR-2 is tele-operated via a wireless LAN (Local Area Network). Table 1 shows the degrees of freedom and dimensions of KHR-2.

2.2 Control System Architecture

The control system architecture of KHR-2 is a distributed control system. The main computer is installed in the torso, and sub-controllers such as joint motor controllers and sensory devices are distributed throughout the body. The communication between the main computer and the sub-controllers is achieved by using a CAN (Controller Area Network) protocol as shown in Fig. 2. The specifications and descriptions of the sub-controllers including sensors are briefly presented in Table 2 [5].

2.3 Motion Control Architecture

The motion control architecture of KHR-2 is completely based on joint position control. Figure 3 shows the motion control process. The motion generator generates the positions of end effectors in Cartesian space. All joint trajectories are generated through inverse kinematics and they are transmitted to the joint motor controllers via the CAN protocol. The

Table 1 Degrees of freedom and dimensions of KHR-2

Dimensions of the biped humanoid robot				
Head	Eye (pan & tilt)		2 DOF×2=4 DOF	
	Neck (pan & tilt)		2 DOF	
Arm	Shoulder (roll/pitch/yaw)		3 DOF×2=6 DOF	
	Elbow (pitch)		1 DOF×2=2 DOF	
Hand	Wrist (roll/pitch)		2 DOF×2=4 DOF	
	Finger		1DOF×5×2=10 DOF	
Torso	Waist (yaw)		1 DOF	
Leg	Hip (roll/pitch/yaw)		3 DOF×2=6 DOF	
	Knee (pitch)		1 DOF×2=2 DOF	
	Ankle (roll/pitch)		2 DOF×2=4 DOF	
Total			41 DOF	
Dimensions (mm)	Height	1,200	Length of upper leg	290
	Width (Shoulder to shoulder)	420	Length of lower leg	280
	Depth (Chest to back)	213	Length between hip joints	142
	Length of upper arm	184	Width of sole	140
	Length of lower arm	185.5	Length of sole	233

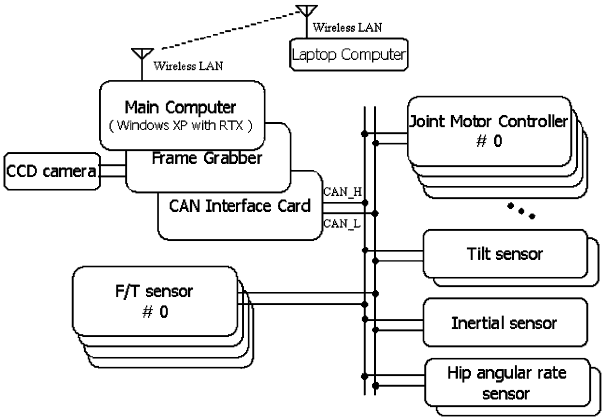

Fig. 2 Overall system configuration of KHR-2

joint motor controllers control the joint positions by using PD controllers with a linear interpolation at 1 kHz.

3 Adjustment Algorithm

Adjustment of our humanoid robot is performed by four kinds of controllers using the inertial sensor and force torque sensors. They are the ZMP Regulation Controller (ZRC), Orientation Correction Controller (OCC), Compliance Controller (CC) on the roll joint of the ankle and Ankle Torque Difference Controller (ATDC). It is important to note that these controllers are activated simultaneously not one by one. The adjustment process is performed once before walking. After the completion of adjustment process, it is not necessary to repeat the adjustment. As a result of adjustment, offset values of the four controllers are derived. If we add the offsets to the reference position in the Cartesian space or joint space, we can minimize the difference between real and experimental conditions and obtain good walking performance. For an ideal floor which is perfectly flat and perpendicular to the gravity, the authors proposed using the Balance Plate as shown in Fig. 4. It has three supports and a level meter so that an ideal floor can be easily achieved. During the adjustment process, the robot stands on the Balance Plate in double support. After the adjustment, the robot comes down on the real ground.

Table 2 Sub-controllers of KHR-2

Item	Description
Joint motor controller	DC servo motor control (400W/ch or 48W/ch)
Force/torque sensor	Measurement of ground reaction forces (one normal force up to 1,000 N and two moments up to 60 Nm)
Inertial sensor	Measurement of roll and pitch inclinations (up to ±15°) of the torso using rate gyros (up to ±100°/s) and accelerometers (up to ±2 g)
Tilt sensor	Measurement of ground roll and pitch inclination (up to ±15°) and Forward and lateral acceleration (up to ±2 g) of foot
Hip angular rate sensor	Measurement of roll angular velocities (up to ±100°/s) of right and left hip

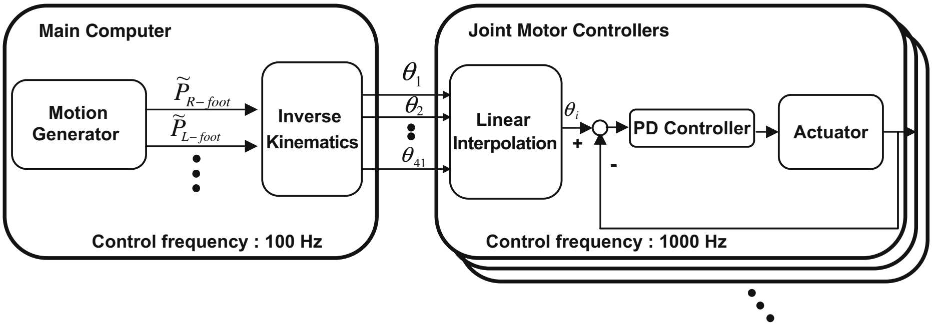

Fig. 3 The motion control process of KHR-2

3.1 ZMP Regulation Controller (ZRC)

As a ready posture for walking, powered robots usually hold the posture as shown in Fig. 5, where the robot is bending its knees a little and keeping the pelvis at constant height. The actual ZMP with respect to OXYZ which is fixed at the center position between the two feet on the ground is calculated from the force/torque sensors integrated with the sole of the foot [7]. We assume that the robot is holding the home posture of Fig. 5 on the perfect horizontal floor of Fig. 4. Here, the measured ZMP should be located at a specific point which is calculated from the ideal model, but, in reality, the measured ZMP has a deviation from the specific point because of the accumulated absolute angle error of several joints. In other words, there exist offsets of the pelvis center point along the X and Y axes in the real environment with respect to the OXYZ frame. In this situation, the ZMP regulation controller (ZRC) is useful in finding offsets in the transverse plane. By feedback from a measured ZMP using the force/torque sensors, the ZRC modifies the pelvis center position in the Cartesian space of OXYZ.

In order to compensate the deviation between the ideal and actual ZMP, we designed a ZMP regulation controller. The control objective is to regulate the measured ZMP at the ideal ZMP zero by changing the pelvis offset position while keeping its height constant. In order to satisfy this objective, there are several different strategies; a control strategy using COG Jacobian [12], a torso position compliance control strategy [13] which tracks a given ZMP trajectory and so on. Currently, our strategy is based on the following full state

Fig. 4 Photograph of the balance plate

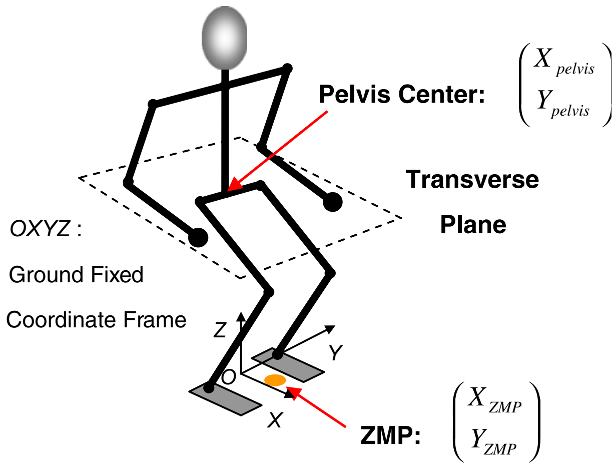

Fig. 5 Schematics of home posture (walking ready posture) and ZMP regulation controller

feedback controller with integral control. In double support phase, we can assume the robot is a simple 2D inverted pendulum with a compliant joint. In Fig. 6, m is the point mass, l is the link length, K is the spring constant, g is the gravitational acceleration, T is the torque from ground reaction force, θ_{des} and θ_{act} are the desired joint angle and the actual joint angle, x_{des} and x_{act} are the desired displacement and the actual displacement of the point mass on the horizontal plane, and x_{ZMP} is the ZMP. The equation of motion of the model can be written as follows;

$$ml^2\ddot{\theta}_{\mathrm{act}} = -K(\theta_{\mathrm{act}} - \theta_{\mathrm{des}}) + mgl\,\sin\,\theta_{\mathrm{act}} \tag{1}$$

Here, if we assume that θ_{des} and θ_{act} are small, θ_{des} and θ_{act} are equal to θ_{des}/l and θ_{act}/l respectively. We can derive a transfer function as follows by using Laplace transform.

$$\frac{X_{\mathrm{act}}(s)}{X_{\mathrm{des}}(s)} = \frac{\frac{K}{ml^2}}{s^2 + \frac{K}{ml^2} - \frac{g}{l}} \tag{2}$$

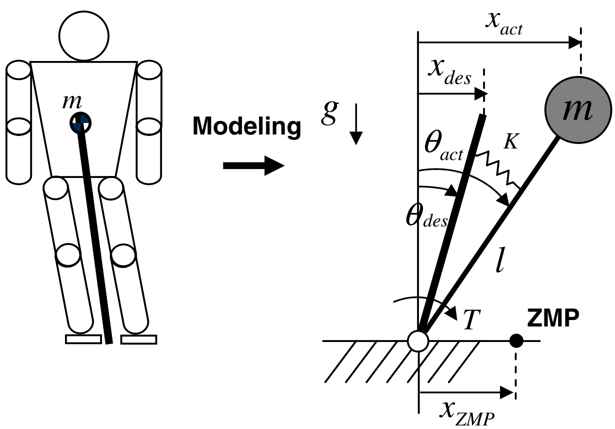

Fig. 6 Mathematical model of the robot in the double support phase

Moreover, a ZMP dynamic equation of a simple 2D inverted pendulum is

$$x_{\mathrm{ZMP}} = x_{\mathrm{act}} - \frac{l}{g}\ddot{x}_{\mathrm{act}} \tag{3}$$

Finally, we can get a transfer function between ZMP and the desired displacement of the point mass on the horizontal plane as

$$\frac{X_{\mathrm{ZMP}}(s)}{X_{\mathrm{des}}(s)} = \frac{K}{mgl} \cdot \frac{-s^2 + \frac{g}{l}}{s^2 + \left(\frac{K}{ml^2} - \frac{g}{l}\right)} \tag{4}$$

In this model, we easily identified unknown variables K and l by a step response and free vibration response in real experiments. For a ZMP regulation controller (ZRC), we designed a full state feedback controller with an integral control and built a control block diagram as shown in Fig. 7. In Fig. 7, the second order compensator, $C(s)$, is composed of full state feedback controller with a full state observer, and the leaking integrator, $H(s)$, is a first order low pass filter with a proper gain. The cutoff frequency of $H(s)$ was experimentally determined by hand tuning and a trade-off between the response time and maximum controllable range.

The ZRC was applied for both x and y components of ZMP in the sagittal and coronal plane to make the measured ZMP to converge into the desired ZMP. During adjustment, external forces and disturbances should not be applied to the robot. After the measured ZMP is converged to the desired ZMP, the control inputs, $X_{\mathrm{pelvis}}^{\mathrm{offset\,ZRC}}$ and $Y_{\mathrm{pelvis}}^{\mathrm{offset\,ZRC}}$ are saved as the pelvis offsets for the adjustment of the home posture. Finally, these offsets are added to the original pelvis trajectories during walking as Eqs. 5 and 6.

$$X_{\mathrm{pelvis}}^{\mathrm{adjusted}} = X_{\mathrm{pelvis}}^{\mathrm{original}} + X_{\mathrm{pelvis}}^{\mathrm{offset\,ZRC}} \tag{5}$$

$$Y_{\mathrm{pelvis}}^{\mathrm{adjusted}} = Y_{\mathrm{pelvis}}^{\mathrm{original}} + Y_{\mathrm{pelvis}}^{\mathrm{offset\,ZRC}} \tag{6}$$

3.2 Orientation Correction Controller (OCC)

When a robot holds a pose as shown in Fig. 1 on a flat floor perpendicular to gravity, the roll and pitch orientation of the torso may deviate from the ideal zero because of an inaccuracy of zero positions of joints. Therefore an orientation correction controller is introduced to correct the pitch and roll angle of the torso in both the sagittal and coronal planes. In the sagittal plane, the controller corrects the pose by measuring the pitch angle with the inertial sensor measuring the direction of gravity and changing the pitch angle of

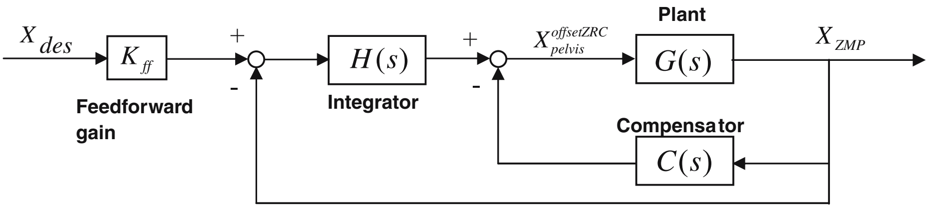

Fig. 7 Control block diagram of ZMP regulation controller(ZRC) for X-axis

the ankle during adjustment. We can also use the pitch angle of the hip, but eventually the result will be same because other controllers are also activating. In the coronal plane, the orientation correction controller corrects the pose by measuring the roll angle of the torso and changing the relative leg length of the left and right legs. During this controller, the ZRC regulates ZMP as well. Here, the leg length means the length between hip joint and ankle joint along Z-axis. Figure 8 shows the action of the orientation correction controller. At the pitch angle of the ankle, the orientation correction controller superimposes the control input of Eq. 7 on the original ankle position as follows:

$$\theta_{\text{ankle pitch all}}^{\text{offset OCC}} = -\left(K_{\text{P}} + \frac{K_{\text{I}}}{s}\right)\theta_{\text{pitch error}}^{\text{torso}} \tag{7}$$

$$\theta_{\text{ankle pitch L}}^{\text{adjusted}} = \theta_{\text{ankle pitch L}}^{\text{original}} + \theta_{\text{ankle pitch all}}^{\text{offset OCC}} \tag{8}$$

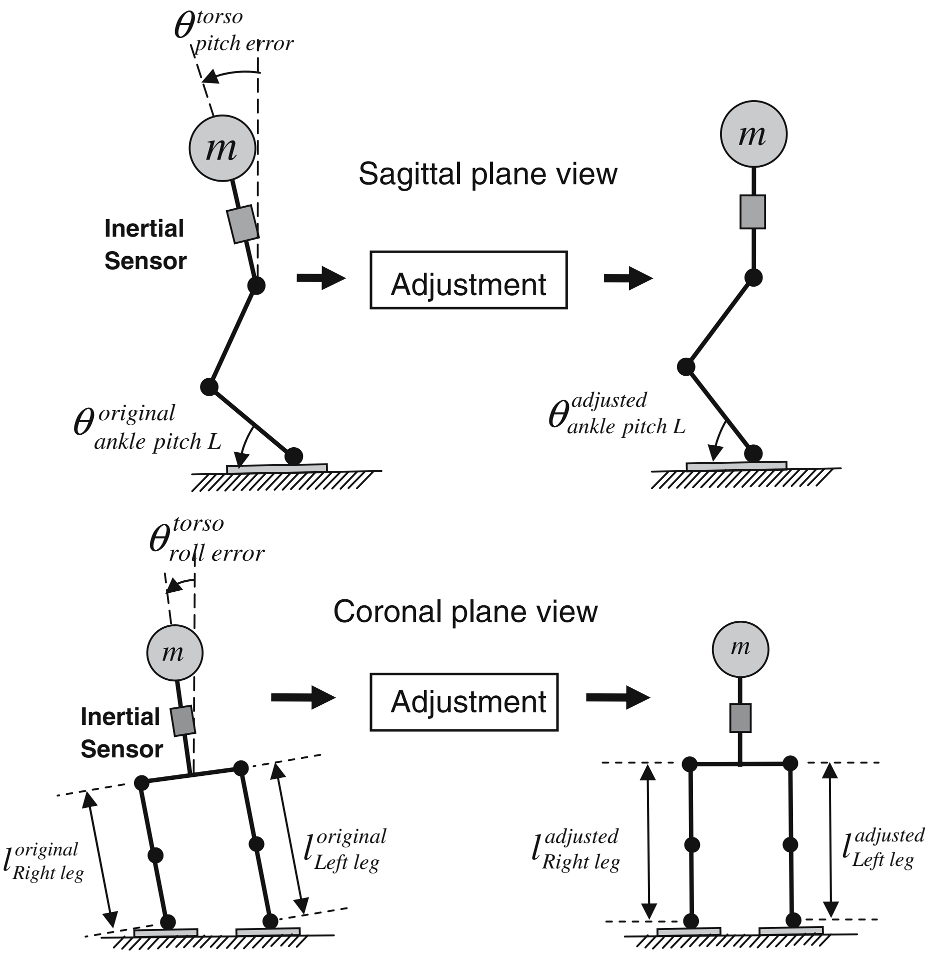

Fig. 8 Action of orientation correction controller

$$\theta_{\text{ankle pitch R}}^{\text{adjusted}} = \theta_{\text{ankle pitch R}}^{\text{original}} + \theta_{\text{ankle pitch all}}^{\text{offset OCC}} \tag{9}$$

where, KP and KI are the proportional and the integral gains of PI controller and this control is performed on both left and right ankle joint during adjustment process.

The roll angle of the robot is adjusted by changing the relative leg length. The orientation correction controller finds the offsets of the leg length by a PI feedback control rule with the torso roll error $\theta_{\text{roll error}}^{\text{torso}}$ as input. Then, the adjusted right leg length is calculated by adding this offset to the original leg length and the adjusted left leg length is calculated by subtracting the offset from the original leg length. The following equations represent the control law.

$$l_{\text{Leg}}^{\text{offset OCC}} = -\left(K_{\text{P}} + \frac{K_{\text{I}}}{s}\right)\theta_{\text{roll error}}^{\text{torso}} \tag{10}$$

$$l_{\text{Right Leg}}^{\text{adjusted}} = l_{\text{Right Leg}}^{\text{original}} + l_{\text{Leg}}^{\text{offset OCC}} \tag{11}$$

$$l_{\text{Left Leg}}^{\text{adjusted}} = l_{\text{Left Leg}}^{\text{original}} - l_{\text{Leg}}^{\text{offset OCC}} \tag{12}$$

where, K_{P} and K_{I} are the proportional and integral gains of PI controller. In this manner, we can make the offsets that enable the robot to keep its torso upright against the global inclination of the floor before operating walking.

3.3 Compliance Controller for the Roll Joint of the Ankle (CC)

During adjustment by the orientation correction controller, position control of the roll joint of the two ankles is disabled in order to move freely against the external torque. In case of KHR (KAIST Humanoid Robot) series, the backdrivability of the ankle joint is good. This fact means that the torque of the roll joint on the ankle is nearly zero during adjustment and its backdrivability does not affect the convergence of the adjustment process. However, when a robot has a non-backdrivable roll joint on the ankle, the roll joint cannot be moved by an external torque even though the position control is off. As a result of non-backdrivability, undesirable torque occurs between the foot and ground along the roll axis. In this case, it is necessary to actively control the ankle to make its torque zero. This compliance control at the roll ankle joint is expressed as the following equation.

$$\begin{cases} \textit{for non}-\textit{backdrivable joint}: \\ \qquad \theta_{\textit{ankle roll L}}^{\textit{offset CC}} = \frac{T_{\textit{roll L}}}{Cs+K} \\ \textit{or backdrivable joint}: \text{ in this case, position control is turned off and the measured} \\ \text{encoder error is set to the offset.} \end{cases} \tag{13}$$

$$\theta_{\text{ankle roll L}}^{\text{offset CC}} = \theta_{\text{ankle roll L}}^{\text{Encoder Error from initial angle}} \tag{14}$$

$$\theta_{\text{ankle roll L}}^{\text{adjusted}} = \theta_{\text{ankle roll L}}^{\text{original}} + \theta_{\text{ankle roll L}}^{\text{offset CC}} \tag{15}$$

The compliance control on the right ankle joint can be expressed in the same manner with an independent controller, where, $T_{\text{roll L}}$ is the measured torque at the roll joint of the left ankle, C and K are tuning parameters that create the satisfactory backdrivability around the roll joint of the ankle. For the adjustment process of Hubo FX-1 [14], the above compliance control algorithm was indispensable since overall convergence was affected by backdrivability.

3.4 Ankle Torque Difference Controller (ATDC)

During adjustment, there is a possibility that the feet of the robot do not fully contact the ground even though ZMP and pose converge to the desired value. This imperfect contact with the ground can be confirmed by observing the roll and pitch torques of the F/T sensors. As the roll ankle joints are free, we can assume that only the pitch angle of the ankle has imperfect contact. Torques of the pitch ankle axes could be different on the two feet. The ankle torque difference controller makes the two torque values on the pitch ankles equal. The authors applied a PI controller which uses the torque difference between the two pitch ankle joints as an input. The equation of the ankle torque difference controller is expressed as follows.

$$\theta_{\text{ankle pitch L}}^{\text{offset ATDC}} = -\left(K_{\text{p}} + \frac{K_{\text{I}}}{s}\right) \times \left(T_{\text{pitch R}} - T_{\text{pitch L}}\right) \tag{16}$$

where, $T_{\text{pitch R}}$ and $T_{\text{pitch L}}$ is the measured torques at right and left pitch joints of ankles. Finally, adding the above offset to Eqs. 8, 9 becomes following equations.

$$\theta_{\text{ankle pitch L}}^{\text{adjusted}} = \theta_{\text{ankle pitch L}}^{\text{original}} + \theta_{\text{ankle pitch all}}^{\text{offset OCC}} + \theta_{\text{ankle pitch L}}^{\text{offset ATDC}} \tag{17}$$

$$\theta_{\text{ankle pitch R}}^{\text{adjusted}} = \theta_{\text{ankle pitch R}}^{\text{original}} + \theta_{\text{ankle pitch all}}^{\text{offset OCC}} \tag{18}$$

It is important to note that the authors do not make both pitch torques zero. We only make the torque difference zero so that the two ankle torques automatically converge to some value which corresponds to XZMP, the reference of ZMP regulation controller.

Summarizing the algorithms of section III, a schematic diagram of the adjustment process is shown in Fig. 9. The robot system is a MIMO system and the measured input vector and output vector are as follows.

Input vector of adjustment:

$$\theta_{\text{pitch error}}^{\text{torso}}, \theta_{\text{roll error}}^{\text{torso}}, T_{\text{roll L/R}}, T_{\text{pitch L/R}}, X_{\text{ZMP}}^{\text{error}}, Y_{\text{ZMP}}^{\text{error}}$$

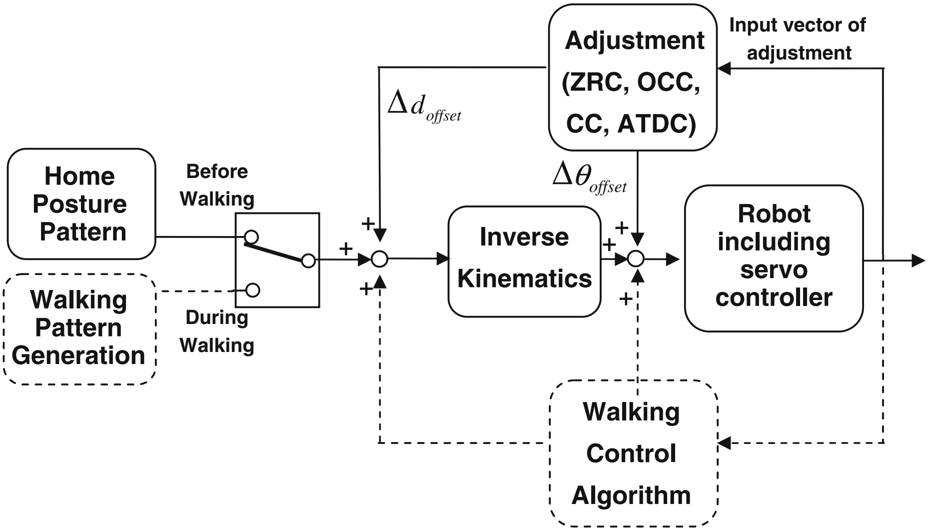

Fig. 9 Schematic diagram of adjustment algorithms

Output vector of adjustment:

$$\begin{cases} \text{Displacement } \Delta d_{offset} : X_{ZMP}^{offset\ ZRC}, \quad Y_{ZMP}^{offset\ ZRC}, \quad l_{Leg}^{offset\ OCC} \\ \text{Orientation } \quad \Delta\theta_{offset} : \theta_{ankle\ pitch\ L}^{offset\ ATDC}, \quad \theta_{ankle\ pitch\ all}^{offset\ OCC}, \theta_{ankle\ roll\ L/R}^{offset\ CC} \end{cases}$$

When all the outputs have converged, the offsets for the position, orientation and relative leg length are determined. After the adjustment process, the displacement offsets are added before the inverse kinematics block and the orientation offsets are added after the inverse kinematics block when the robot walks. The Fig. 9 shows how the robot adjusts its home posture and improves its walking performance when the initial home posture errors exist.

4 Experiments

To demonstrate the effectiveness of our approach, we conducted the adjustment process on KHR-2. Before the experiment, zero positions of each joint of the lower body were set by hand. By position control using inverse kinematics, the robot attained the home posture as shown in Fig. 1. First, we tested the adjustment algorithm by analyzing sensory data and control inputs. Second, we also tested the effectiveness of the adjustment through walking experiments using KHR-2.

4.1 Adjustment Algorithm Experiment

After the robot stands on the Balance Plate with the home posture, we activated the proposed adjustment algorithm after a while. An abrupt start of control input can be avoided, if we activate the adjustment after the force/ torque sensor and inertial sensor have steady state values. It is important to note that all controllers of the adjustment algorithm

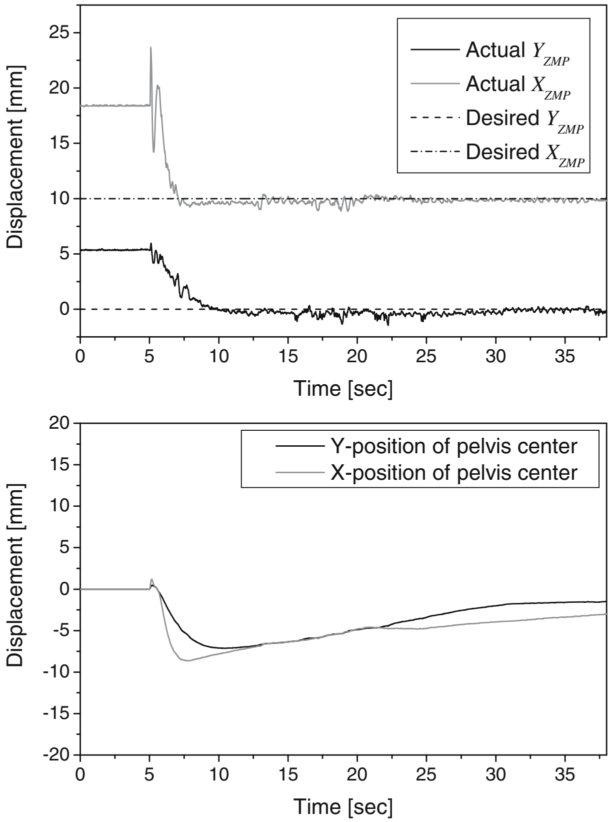

Fig. 10 Experimental results of ZMP regulation controller

were activated simultaneously. As for the ZMP regulation controller, desired XZMP and YZMP are +10 and 0 mm, respectively. Figure 10 shows the experimental results of the ZMP regulation controller. Since there always exists offset between actual pelvis center and ideal pelvis center, initial ZMP values in the graph are arbitrary. When we applied control, it was observed that the actual ZMP values measured by the force/torque sensor are regulated well. X and Y components of the pelvis center with respect to the ground fixed coordinate frame are changing continuously even though ZMP converged to desired value. This is because other controllers are working together.

Figure 11 shows experimental results of the orientation correction controller. Since, at the beginning, the robot's upper body was not adjusted, upper body is inclined a little. This small inclination can also have bad effects on the robot's stable walking. In general, if the robot walks stably, its inclination is within one degree. Therefore, even a small inclination of less than one degree may generate instability. In the graph, it is observed that the roll and pitch angle of the upper body gradually converges to zero when the controller is applied. Leg lengths and ankle pitch angles of both legs are changing slowly.

Figure 12 shows the experimental results of the ankle torque difference controller. Since the robot stood on the ideal ground made by the Balance Plate, an initial difference of torque between both ankle pitch joints was produced due to the incorrect initial positions of ankle pitch joints. When the controller was applied, the torque difference became zero quickly. By using this controller, we can make soles parallel to the ideal ground with ease.

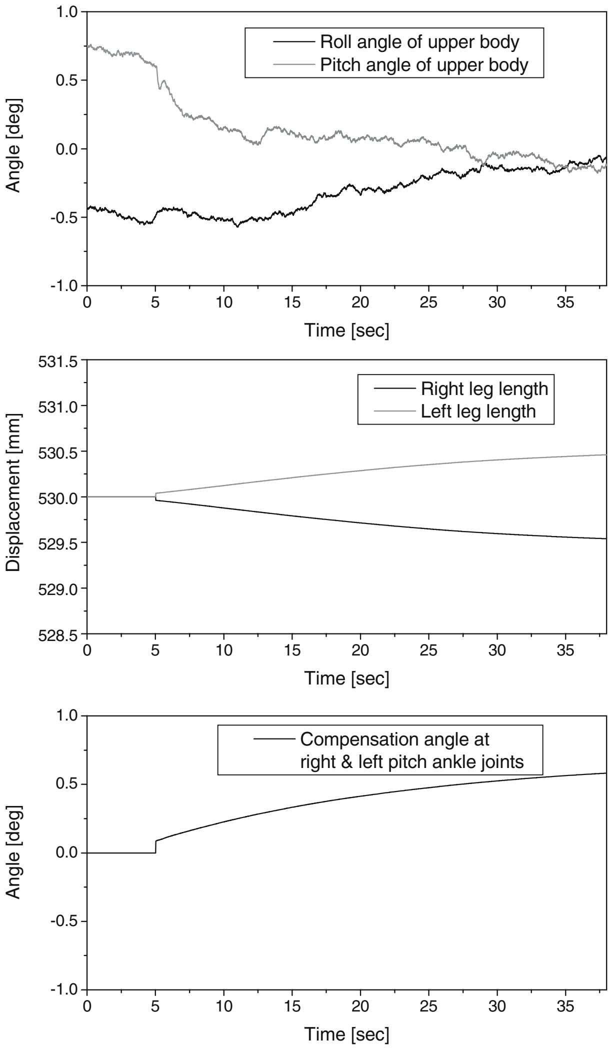

Fig. 11 Experimental results of orientation correction controller

If the pitch angles of both feet are different, the walking motion along the pitch axis is not balanced when it walks.

4.2 Walking Experiment

We also conducted walking experiments using KHR-2. For the biped walking control strategy, we used the algorithms that have been developed by the authors [4, 5]. The objective of the experiment is to evaluate the walking performance before and after adjustment when the robot walks in place. Before adjustment, we set initial angles of the joints by hand. When the robot walks, we measured upper body inclination and ZMP by using the inertial sensor and force torque sensors. Figure 13 shows the experimental results of walking in place before the adjustment. Basically, upper body inclination is changing a

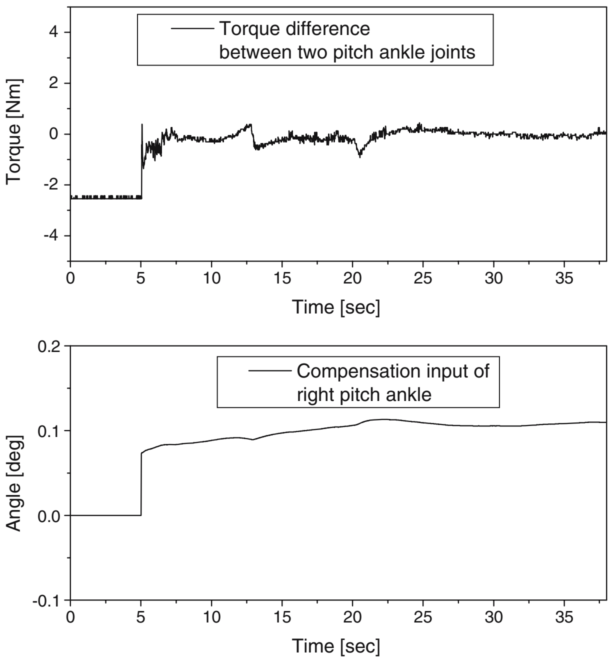

Fig. 12 Experimental results of ankle torque difference controller

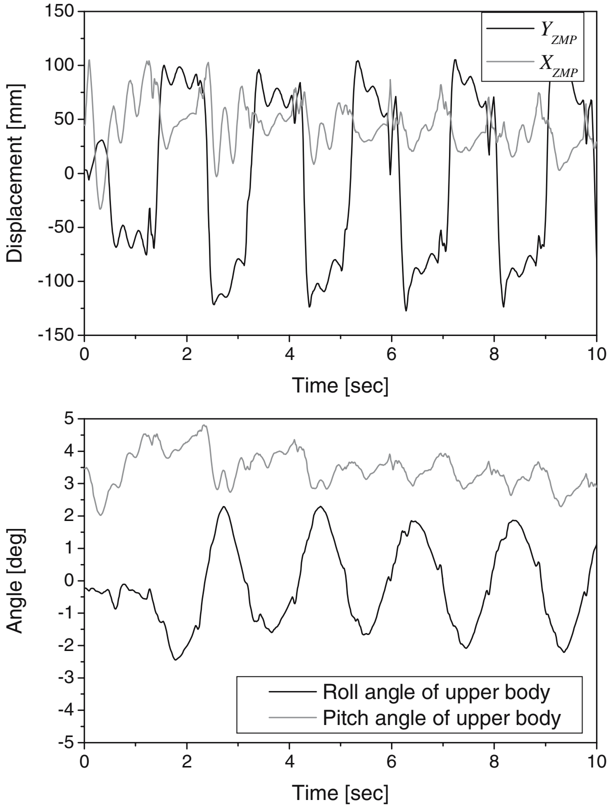

Fig. 13 Experimental results of walking in place before the adjustment

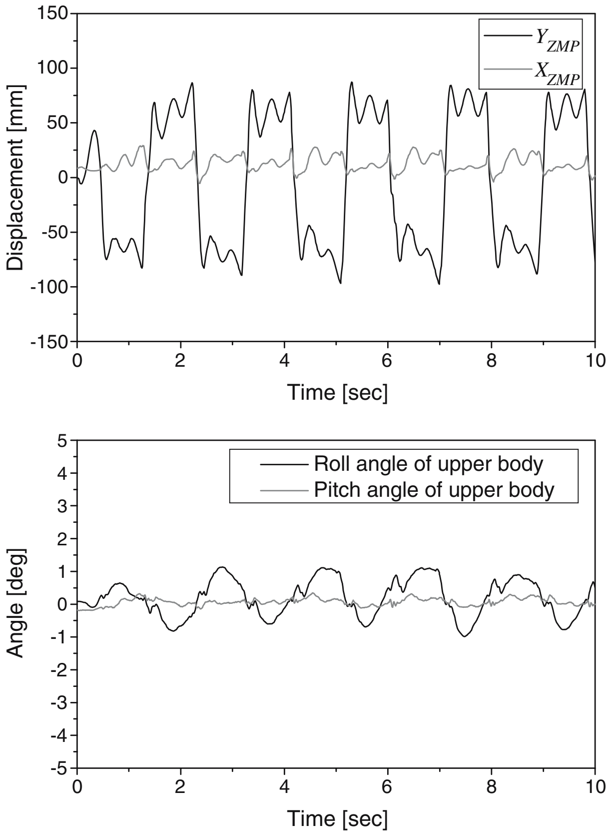

Fig. 14 Experimental results of walking in place after the adjustment

lot, where the range of the roll angle is from −2.4 to +2.3° and that of the pitch angle is from 2 to 4.8°. Neither initial pitch angle nor initial XZMP is near zero. These errors make the robot unstable during walking. Even though an initial roll angle and initial YZMP are well-balanced and near zero, they begin to be excited by the unstable pitch motion and other factors. Figure 14 shows the experimental data when the KHR-2 is walking after adjustment. As a result of the adjustment, the initial pitch and roll angle are almost zero, and the initial XZMP and YZMP are 10 and 0 mm respectively. While the robot walks in place, the roll angle of the torso changes from approximately −1 to 1°. The pitch angle is near zero, where the range within ±0.3°. XZMP and YZMP are also well-balanced within the stable range. The robot is walking very stably after adjustment. In these experiments, we

Table 3 The range and RMS value of inertial sensor and ZMP

	Before adjustment			After adjustment		
	Min.	Max.	RMS	Min.	Max.	RMS
Pitch angle (deg)	2.02	4.81	3.49	−0.18	0.35	0.13
Roll angle (deg)	−2.44	2.26	1.29	−0.98	1.13	0.61
XZMP(mm)	−33.2	105.0	49.29	−5.5	29.2	14.28
YZMP(mm)	−127.4	104.4	77.67	−97.6	87.3	61.77

could confirm the proper working of the proposed adjustment algorithm and prove its effectiveness. The range and RMS value of the inertial sensor and ZMP during the experiment was summarized in the Table 3.

5 Conclusion

In this paper we proposed an adjustment algorithm for the home posture of a biped humanoid robot. The algorithm is composed of four controllers: ZMP regulation controller, orientation correction controller, compliance controller and ankle torque difference controller. As we can see the experimental results in this paper, our adjustment algorithm has been successfully demonstrated on KHR-2. In fact, we have successfully applied the proposed algorithm for all KHR (KAIST Humanoid Robot) series including Hubo FX-1. This fact shows the usability and robustness of the proposed algorithm. Moreover, the algorithm is not complicated and is so effective that we can easily apply it to many different biped humanoid robots. Though the adjustment process needs about one minute for convergence, it can guarantee a consistent initial posture before walking. Accordingly, the authors can always analyze and design biped walking controllers effectively with a constant initial posture. It can be thought that a consistent initial posture can be realized through the use of an absolute position measurement such as potentiometers, limit switches and index pulses of the incremental encoders. However, it is still necessary to apply the calibration process once to the system. With the absolute position measurement, it is hard to determine the appropriate zero positions of multiple joints, and it is hard to consider the change of the zero position due to the gradual mechanical deformations or assembly variations at every experiment. In other words, a problem is to determine where the zero position of each joint must be placed at every experiment under the environment variations. To solve this problem, the absolute position measurement is not sufficient. Furthermore, the absolute position measurement makes the robot design complicated. Therefore, we developed an automatic adjustment algorithm with only incremental encoders. Though the proposed algorithm should be performed after every start-up, it always provides an accurate home posture.

At this moment, only the joints of lower body of the biped robot are adjusted. This is because the adjustment of the lower body is more important than the upper body in terms of accurate inverse kinematics during walking. In fact, the upper body pose affects the adjustment of the lower body. So, the development of an efficient adjustment algorithm for the upper body of a humanoid robot is future work.

Acknowledgement This work was supported by research fund of Myongji University.

References

1. Hirai, K., Hirose, M., Haikawa, Y., Takenaka T.: The development of Honda humanoid robot. In: Proc. of Int. Conf. on Robotics and Automations, 1321–1326 (1998)
2. Kim, J.-H., Park, S.-W., Park, I.-W., Oh, J.-H.: Development of a humanoid biped walking robot platform KHR-1 – initial design and its performance evaluation. In: Proc. of 3rd IARP Int. Workshop on Humanoid and Human Friendly Robotics, Tsukuba, 14–21 (2002)
3. Kim, J.–H., Oh, J.-H.: Torque feedback control of the humanoid platform KHR-1. In: Proc. of 3rd IEEE Int. Conf. on Humanoid Robots, Karlsruhe and Munich, Germany (2003)
4. Kim, J.-H., Oh, J.-H.: Realization of dynamic walking for the humanoid platform KHR-1. Adv. Robot. **18**, (7), 749–768 (2004)

5. Kim, J.-Y., Park, I.-W., Lee, J., Kim, M.-S., Cho, B.-K., Oh, J.-H.: System design and dynamic walking of humanoid robot KHR-2. In: Proc. IEEE Int. Conf. on Robotics & Automation, 1431–1436 (2005)
6. Park, I.-W., Kim, J.-Y., Lee, J., Oh, J.-H.: Mechanical design of humanoid robot platform KHR-3 (KAIST Humanoid Robot-3: HUBO). In: Proc. IEEE/RAS Int. Conf. on Humanoid Robots, 321–326 (2005)
7. Vukobratovic, M., Borovac, B., Surla, D., Stokic, D.: Biped locomotion: dynamics, stability, control and application. Springer-Verlag, New York (1990)
8. Legnani, G., Mina, C., Trevelyan, J.: Static calibration of industrial manipulators design of an optical instrumentation and application to SCARA robots. J. Robot. Syst. **13**, (7), 445–460 (1996)
9. Driels, M.R., Swayze, W.E.: Automated partial pose measurement system for manipulator calibration experiments. IEEE Trans. Robot. Autom. **10**, (4), 430–440 (1994)
10. Canepa, G., Hollerbach, J.M., Boelen, A.J.M.A.: Kinematic calibration by means of a triaxial accelerometer. In: Proc. of Int. Conf. on Robotics and Automations, 2776–2782 (1994)
11. Gonzalez de Santos, P., Jiménez, M.A., Armada, M.A.: Improving the motion of walking machines by autonomous kinematic calibration. Auton. Robots **12**, (2), 187–199 (2002)
12. Sugihara, T., Nakamura, Y.: Whole-body cooperative balancing of humanoid robot using COG Jacobian. In: Proc. Int. Conf. on Intelligent Robots and Systems, 2575–2580 (2002)
13. Nagasaka, K., Inaba, M., Inoue, H.: Stabilization of dynamic walk on a humanoid using torso position compliance control. In: Proc. 17th Annual Conference on Robotics Society of Japan, 1193–1194 (1999)
14. Kim, J.-Y., Lee, J., Oh, J.-H.: Experimental realization of dynamic walking for a human-riding biped robot, HUBO FX-1. Adv. Robot. **21**, (3), 461–484 (2007)